ACS OMEGA

Open Access

http://pubs.acs.org/journal/acsodf

Article

Significantly High Melting Temperature of Homopolymer Crystals Obtained in a Poly(L-Lactic Acid)/Poly(D-Lactic Acid) (50/50) Blend

Neimatallah Hosni Mohammed Mahmoud, Hideaki Takagi, Nobutaka Shimizu, Noriyuki Igarashi, and Shinichi Sakurai*

Cite This: *ACS Omega* 2023, 8, 40482−40493

Read Online

ACCESS | Metrics & More | Article Recommendations | Supporting Information

ABSTRACT: The isothermal crystallization of a poly(L-lactic acid) (PLLA)/poly(D-lactic acid) (PDLA) (50/50) blend, neat PLLA, and neat PDLA, was studied at different crystallization temperatures (110 °C, 150 °C, 170 and 180 °C) for different durations (1−300 min) by means of differential scanning calorimetry (DSC), polarized optical microscope (POM) observations, and time-resolved wide-angle X-ray diffraction (WAXD). The effects of both the isothermal crystallization temperature and the duration of the isothermal crystallization were investigated for the blend specimens fully crystallized at these crystallization temperatures. The formation of homopolymer crystallites (HC) was confirmed at the isothermal crystallization temperature of 170 °C, which was previously considered too high for its formation, after 70 min had elapsed from the temperature stabilization. Moreover, the melting temperature of the formed HC was found to be significantly high (T_m = 187.5 °C) compared to the one obtained during the nonisothermal DSC measurement of the same specimen of the PLLA/PDLA (50/50) blend, as well as the neat PLLA and PDLA specimens. To the best of our knowledge, this extremely high T_m (=187.5 °C) for HC has never been reported before.

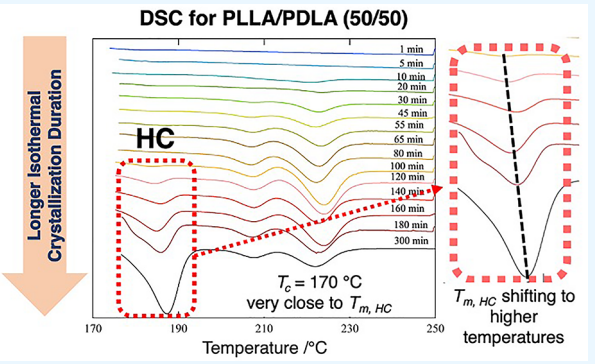

INTRODUCTION

The COVID-19 pandemic caused a significant surge in personal protective equipment waste (e.g., masks, gloves, etc.)[1] and single-use plastics.[2] This highlights the significance of researching environmentally friendly polymers that can replace fossil-fuel-based ones. Polylactic acid (PLA) is an aliphatic polyester produced from renewable agricultural sources and is one of the most researched biobased polymers.[3] Its growing popularity stems from its many favorable qualities, such as biodegradability, nontoxicity, bioabsorbability, and high transparency. Nevertheless, improving its mechanical and thermal properties remains a challenge.

PLA exists in two enantiomeric forms: poly(L-lactic acid) (PLLA) and poly(D-lactic acid) (PDLA). Besides forming homo crystallites (HC), these two enantiomers can form stereocomplex crystallites (SC).[4] The tightly packed SC leads to the improvement of mechanical properties and a melting temperature, which is about 50 °C higher than that of HC.[5] Therefore, promoting the stereocomplexation of PLA is one of the best approaches to ameliorate its poor properties, such as hydrolysis resistance, thermal stability and heat distortion temperature.[6−8] However, the SC formation is usually accompanied by the HC formation.[9] Many studies attempted to form SC exclusively through the addition of nucleation agents[10] or plasticizers,[11,12] the formation of multiarm stereoblock copolymers,[13] and by processing with the aid of ionic liquids.[14]

The relation between SC and HC has been described as competitive by many studies.[15−17] As the melting temperature of HC ($T_{m,HC}$) is lower than that of SC ($T_{m,SC}$), the isothermal crystallization at high temperatures, higher than $T_{m,HC}$ ($T_c > T_{m,HC}$), where T_c denotes the isothermal crystallization temperature, can selectively produce SC. Pan et al. stated that only SC would form at T_c in the range of 170−180 °C.[18] A similar result was obtained by Bao et al.[9] and Pandey et al.[19] where they reported the almost exclusive formation of SC at T_c = 170 °C.

Since the isothermal crystallization duration can improve the degree of crystallinity, to some extent,[20] there is a need to thoroughly examine the effect of different durations in the case of PLLA/PDLA blends. In this study, the crystallization behaviors of a PLLA/PDLA (50/50) blend specimen, neat PLLA, and neat PDLA were examined through isothermal crystallization at different temperatures for different durations.

Received: July 18, 2023
Accepted: September 14, 2023
Published: October 17, 2023

The isothermal crystallization behaviors were studied by means of differential scanning calorimetry (DSC), polarized optical microscope (POM) observations, and time-resolved wide-angle X-ray diffraction (WAXD). The effects of both the temperature and duration of the isothermal crystallization will be discussed. The focus of this study is to confirm the effect of the long crystallization duration at T_c = 170 °C, along which HC formation takes place, compared to shorter crystallization durations. The significance of this finding exists in the unexpected formation of HC at a temperature very close to its presumed melting temperature, and its actual melting temperature is remarkably high.

EXPERIMENTAL SECTION

MATERIALS. PLLA was obtained from NatureWorks LLC, USA (grade 2500 HP) and PDLA was obtained from Purac (grade D130). Table 1 summarizes the materials characterization. Film specimens were prepared by solution casting using dichloromethane (DCM) as solvent from 5% (w/v) of polymer concentration. PLLA and PDLA pellets were weighed in a 1:1 ratio then the solvent was added. The mixture was placed over a magnetic stirrer for 24 h, before being cast in a 5 cm diameter Petri dish for solvent evaporation at room temperature. Both PLLA and PDLA were also used to prepare neat specimens of the homopolymers by following the aforementioned method.

Table 1. Materials Characterization

	PLLA	PDLA
code	2500HP	D130
optical purity	99.5%	>99.5%
number-average molecular weight (M_n) (GPC)[a]	1.74×10^5	1.41×10^5
M_w/M_n (GPC)	2.22	2.03

[a]The GPC column was calibrated using the standard polystyrene with chloroform as eluent at room temperature.

DSC Measurements. DSC measurements for nonisothermal crystallization of the PLLA/PDLA blend specimen were carried out, under a nitrogen atmosphere, using the Shimadzu DSC-60 Plus instrument (Shimadzu, Kyoto, Japan), by the following thermal program. The as-cast specimen was heated from 25 to 250 °C, with a heating rate of 10 °C/min, and maintained for 5 min to erase the thermal history during the casting process. Then, it was cooled to 25 °C at the rate of 10 °C/min. The second-heating run was conducted from 25 to 250 °C at the rate of 10 °C/min.

As for the isothermal crystallization, DSC measurements were carried out, under a nitrogen atmosphere, using NETZSCH DSC214 Polyma (NETZSCH GmbH & Co. Holding, Germany). The apparatus was calibrated using indium, zinc, bismuth, and tin as references before the measurements. The PLLA/PDLA blend, neat PLLA, and neat PDLA specimens were tested by the following thermal program. They were heated from 25 to 250 °C with a heating rate of 10 °C/min and maintained for 5 min to erase the thermal history during the casting process. Then, they were quenched to a given T_c with a cooling rate of approximately 50 °C/min and kept isothermally for different durations. Afterward, the specimens were heated again to 250 °C to observe the melting temperatures after the isothermal crystallization. In order to correct for the effect of heating rate on the melting temperatures, three different heating rates (5 °C, 10, and 20 °C/min) were used for some specimens isothermally crystallized for 300 min. It is noteworthy that the specimen was renewed for each DSC measurement to avoid unfavorable thermal degradation of the specimens, as will be discussed later in the Results and Discussion on "GPC Analysis For The PLLA/PDLA (50/50) Blend Specimen".

WAXD Measurements. Time-resolved WAXD measurements were performed using synchrotron radiation as the X-ray source at beamline BL-6A of Photon Factory at KEK (High-Energy Accelerator Research Organization) in Tsukuba, Japan. The wavelength of the incident X-ray beam was 0.15 nm. The blend specimen was positioned in an aluminum cell and connected to a thermosensor to monitor its temperature throughout the measurement duration. The cell diameter and thickness are 4 and 1 mm, respectively. To seal the specimen in the cell, polyimide (Kapton) tape (DuPont-Toray Co., Ltd., Tokyo, Japan) was used. In order to achieve the temperature jump from 250 °C to T_c, two heater blocks were used. The specimen was melted at 250 °C for 5 min before being immediately transferred to the second heater block, kept at T_c = 170 °C. The WAXD measurement was performed, while making sure that the temperature stabilizes at T_c within a relatively short time (1−3 min) and that temperature fluctuation during the measurement is within ±0.5 °C of T_c. The magnitude of the scattering vector (q) was calibrated using the standard polyethylene. q is defined as, $q = |\boldsymbol{q}| = (4\pi/\lambda)\sin(\theta/2)$, where λ and θ are the wavelength of the X-ray and the scattering angle, respectively. The two-dimensional wide-angle X-ray diffraction (2D-WAXD) images were recorded every 5 s with an X-ray exposure time of 4 s on a Pilatus 100 K (DECTRIS Ltd., Switzerland) as the two-dimensional detector. The 1D WAXD profiles were obtained by taking the sector average of the 2D-WAXD image.

POM Observations. POM observations were conducted using a Nikon Eclipse C*i*-POL POM equipped with a Linkam THMS600 hot stage (Linkam scientific) to observe the growth of spherulites in the PLLA/PDLA blend specimen at T_c = 170 °C. The specimen was positioned between two glass slides and melted at 250 °C for 5 min before being quenched to 170 °C with a cooling rate of 110 °C/min. Then, it was kept isothermally for 300 min before being heated up again to 250 °C to observe the fading of spherulites.

GPC Analysis. Gel permeation chromatography (GPC) analysis was conducted to determine the molecular weight distribution of the PLLA/PDLA blend sample, before and after the isothermal crystallization for 5 h at 170 and 180 °C. Hexafluoroisopropanol (HFIP) was selected as the eluent due to its excellent solubility for the PLLA/PDLA blend sample. To calibrate the GPC column, poly(methyl methacrylate) was utilized as standard. The GPC analysis was performed to ensure any potential thermal degradation.

RESULTS AND DISCUSSION

Nonisothermal DSC Measurement. In Figure 1, the second-heating run, from 25 to 250 °C, of the nonisothermal DSC measurements showed the glass transition temperature (T_g) at 66.5 °C and a single exothermic crystallization peak at 104.7 °C. The endothermic melting peaks appeared at 176.7 °C, ascribed to the melting of HC, and those at 210.4 and 223.4 °C, both ascribed to the melting of SC, with the former SC peak attributed to the melting of smaller SC crystallites compared to the ones melting at higher temperature. In

https://doi.org/10.1021/acsomega.3c05165
ACS Omega 2023, 8, 40482−40493

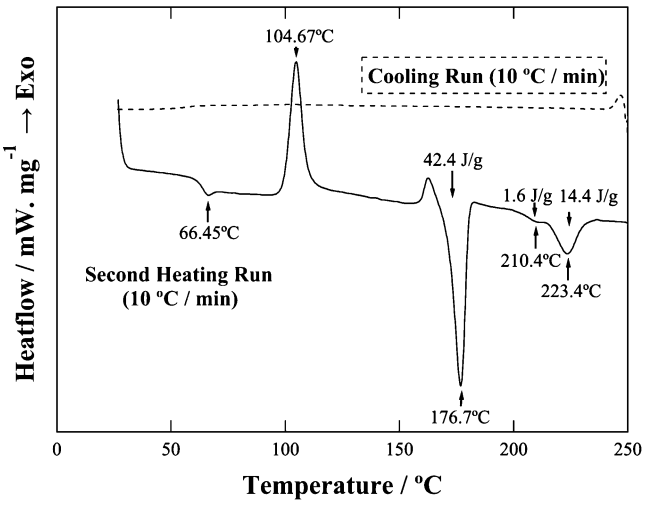

Figure 1. Cooling run and the second-heating run of nonisothermal crystallization of a PLLA/PDLA (50/50) blend specimen.

addition, an exothermic peak is observed at 162.5 °C, which is ascribed to the α' to α transition of HC. The enthalpies of fusion (ΔH_m), calculated by integrating the melting peaks, were 42.41 J/g for the HC, 1.6 J/g for SC_1, and 14.38 J/g for SC_2, whereas the cooling curve shows no crystallization with only a small change in the heat flow around the glass transition temperature. This means that PLA samples used in this study have a low crystallizability. It is worth noting that the second heating run ensured the complete melting of all SC crystallites (erasing of the thermal history of the as-cast specimen) during the 5 min duration at 250 °C before starting the first-cooling run.

Isothermal DSC Measurements of the PLLA/PDLA (50/50) Blend Specimens. The isothermal crystallization measurements of the PLLA/PDLA (50/50) specimens at 110 °C, 150, and 170 °C were performed for different durations of 1, 5, 10, 20, and 30 min, as well as 300 min. For the case of T_c = 170 °C, additional durations were also examined, namely, 45, 55, 65, 80, 100, 120, 140, 160, and 180 min. Figure 2a–c shows the subsequent heating to 250 °C, where T_m is taken at the endothermic peak top and the peaks are assigned to HC, SC_1, or SC_2. SC comprises both SC_1 and SC_2, where SC_1 is for smaller crystallites as compared to SC_2 and, thus, it has a lower melting temperature.

For T_c = 110 °C (Figure 2a), all of the durations showed two melting peaks. HC appeared within 1 min elapsed with a T_m of 173.6 °C that steadily increased to T_m = 176.1 °C after 300 min of isothermal crystallization. For all durations, except 1 min, the HC melting peak was preceded by an exothermic peak, indicating the α' to α transformation of HC. For the duration from 5 to 300 min, this exothermic peak is preceded by a melting peak at T_m of 163.3 and 163.7 °C, respectively. This may indicate the partial melting of α' crystallites before their transformation to α. As for SC_2, its T_m fluctuated between 222.2 °C (after 10 min) and 224.3 °C (after 30 min). On the contrary, SC_1 appeared only after 20 min of isothermal crystallization and its T_m increased steadily from 207.9 °C, after 20 min, to 209.2 °C, after 300 min. As shown in Figures 3a and 5a, the amount of SC_2 ($\Delta H_{m,SC2}$) decreased with an increase in the isothermal crystallization duration at T_c = 110 °C.

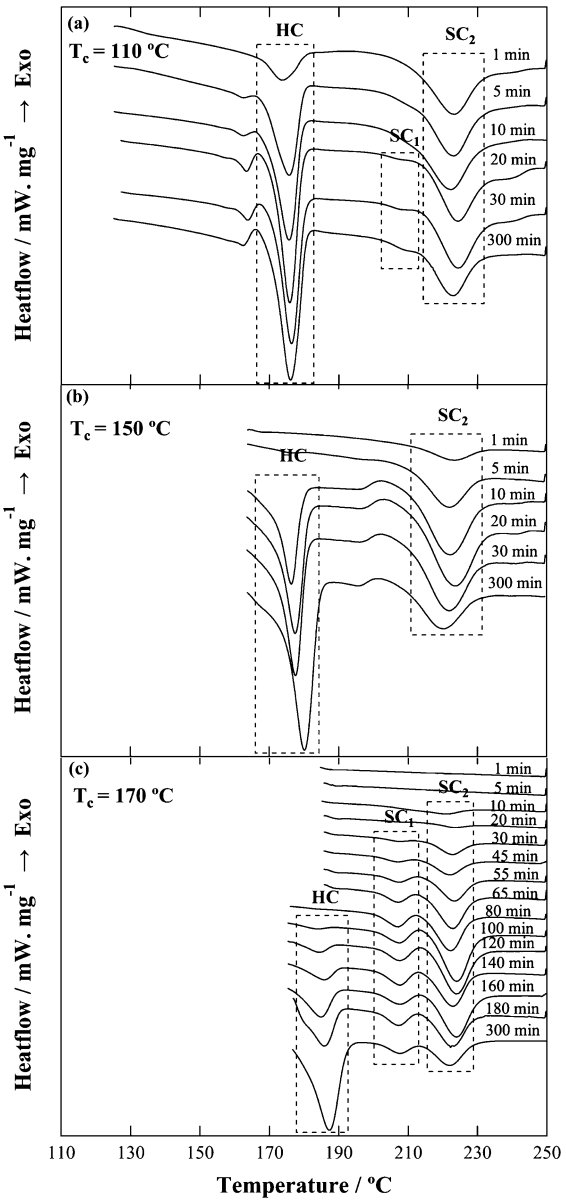

Figure 2. DSC curves during the heating to 250 °C (10 °C/min) after the isothermal crystallization at (a) 110, (b) 150, and (c) 170 °C for the PLLA/PDLA (50/50) blend specimen.

As for T_c = 150 °C (Figure 2b), the shorter crystallization durations, 1 and 5 min, resulted in the exclusive formation of SC_2, exhibiting a single melting peak. This indicates the precedence of SC formation over HC at higher crystallization temperatures compared to T_c = 110 °C. Starting from the crystallization duration of 5 min, HC appeared. The $T_{m,HC}$ followed the same trend as that for the case of T_c = 110 °C, as it started from 176.3 °C (after 10 min) gradually increasing to 180.1 °C (after 300 min). As for the $T_{m,SC2}$, it reached its highest value after 30 min, then gradually decreased to 220.2 °C (after 300 min of the isothermal crystallization). As opposed to the cases of T_c = 110 °C and T_c = 170 °C, a clear melting peak of SC_1 was not observed at T_c = 150 °C; instead, an exothermic peak was clearly observed between HC and SC_2 peaks for the duration of 10 min and longer, presumably indicating a recrystallization process of HC into SC.

Figure 2c presents an interesting result for T_c = 170 °C, showing the DSC curves for additional durations (45, 55, 65,

https://doi.org/10.1021/acsomega.3c05165
ACS Omega 2023, 8, 40482−40493

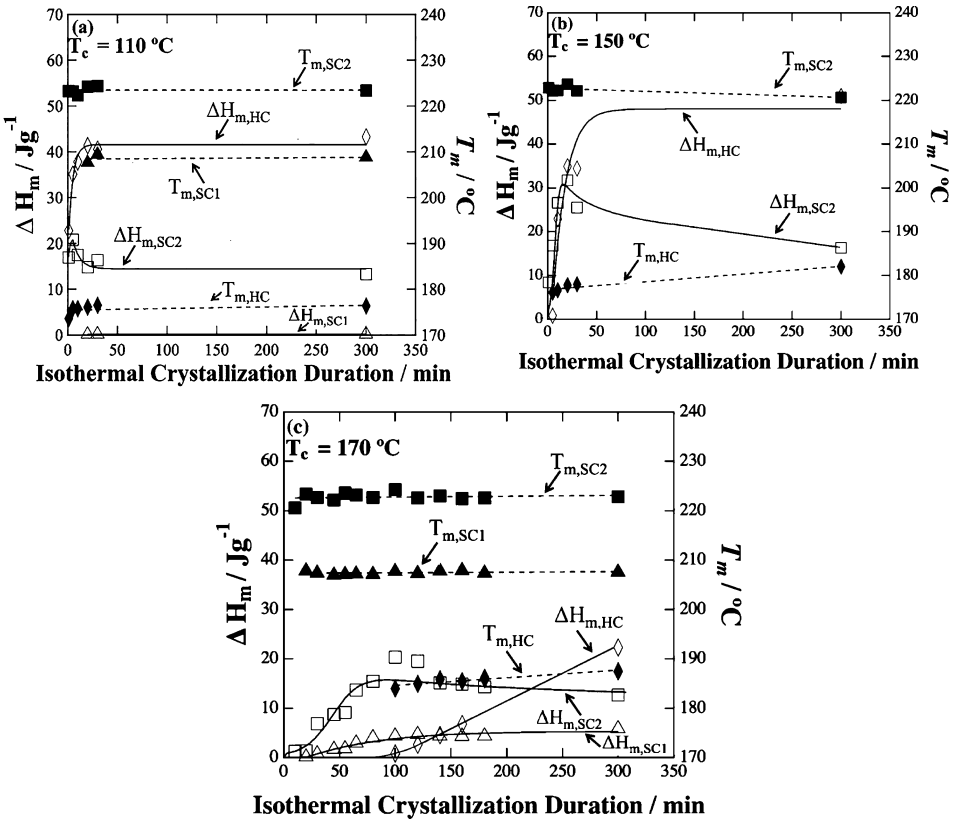

Figure 3. Plots of ΔH_m and T_m of HC, SC_1, and SC_2 as a function of the isothermal crystallization duration at (a) 110, (b) 150, and (c) 170 °C.

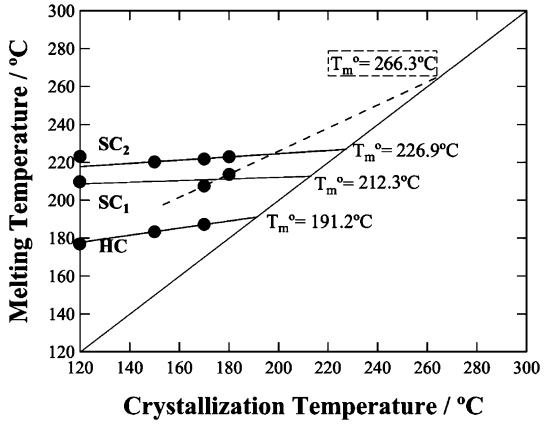

Figure 4. Hoffman–Weeks plots for HC, SC_1, and SC_2.

80, 100, 120, 140, 160, and 180 min), as compared to the other cases of T_c. The induction period was significantly longer compared to the other cases with the first two durations, 1 and 5 min, showing no endothermic peaks, indicating the absence of crystallites. As is the case with T_c = 150 °C, SC formation prevailed in shorter durations with only SC_2 appearing after 10 and 20 min. The durations from 30 to 80 min witnessed the appearance of SC_1 alongside SC_2. Then, HC appeared much later, after a 100 min duration, with a significantly high melting temperature of 184 °C. Furthermore, the longer durations resulted in remarkably high T_m of 186.2 °C (180 min) and 187.5 °C (300 min), which are more than 10 °C higher than the T_m of HC obtained for the same specimen during the nonisothermal DSC measurement (Figure 1) with the same heating rate for the DSC measurement. This T_m is well beyond the common range of HC melting point, namely, 170 °C–180 °C, as reported in the previous studies of PLLA/PDLA 50/50 blends.[12−14] In their review, Saeidlou et al.[21] stated that the melting temperature of PLA increases with molecular weight for low M_n but reaches an asymptotical value at M_n higher than 100 kg/mol. This is in reference to Jamshidi et al.,[22] who reported a T_m of 184 °C for PLLA at infinitely high molecular weight. To the best of our knowledge, the highest melting temperature of HC is 186.5 °C. This result was reported by Nijenhuis et al.[23] for pure PLLA with an extremely high molecular weight of $M_v = 8 \times 10^5$ (M_v: viscosity-average molecular weight).

Figure 3a–c shows the plots of the enthalpy of fusion (ΔH_m) and the melting temperatures (T_m) as a function of the isothermal crystallization duration, where ΔH_m was calculated by integrating the melting peaks of HC, SC_1, and SC_2. T_m and ΔH_m values are presented in Table S1 of the Supporting Information, as well as the percentage of each crystallite type contribution to the overall crystallinity (φ_c), where φ_c was evaluated using the following equations

$$\varphi_{c,HC} = \frac{\Delta H_{m,HC}}{\Delta H_{m^\circ,HC}} \quad (1)$$

$$\varphi_{c,SC} = \frac{\Delta H_{m,SC}}{\Delta H_{m^\circ,SC}} \quad (2)$$

$$\varphi_c = \varphi_{c,HC} + \varphi_{c,SC} \quad (3)$$

$$\Delta H_{m,SC} = \Delta H_{m,SC1} + \Delta H_{m,SC2} \quad (4)$$

where $\Delta H_m^\circ{}_{,HC}$ and $\Delta H_m^\circ{}_{,SC}$ are the enthalpies of fusion of 100% crystal for HC and SC, taken as 93[24] and 142 J/g,[25]

https://doi.org/10.1021/acsomega.3c05165
ACS Omega 2023, 8, 40482−40493

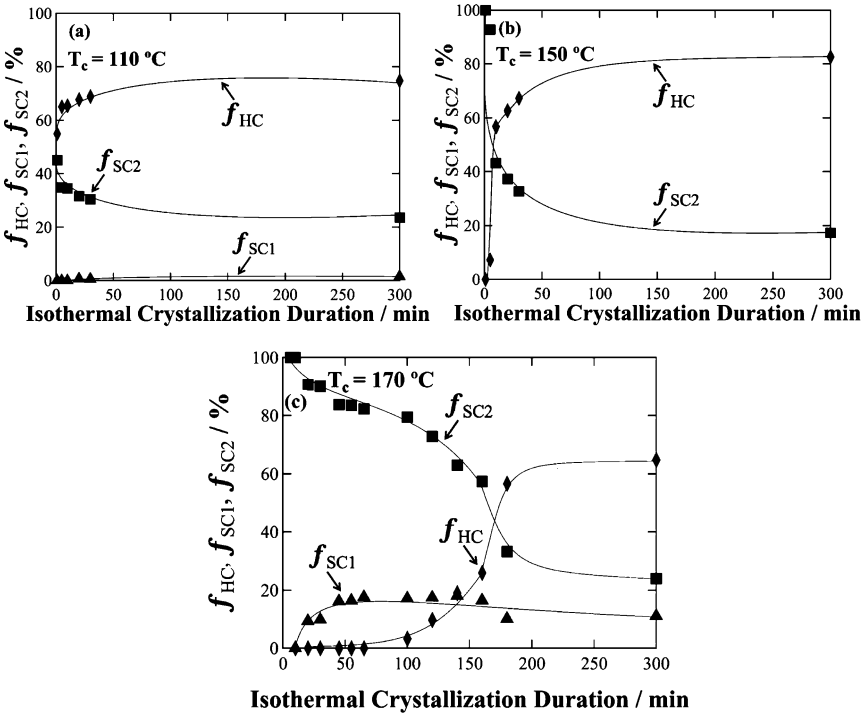

Figure 5. Contributing fractions of HC, SC_1, and SC_2 to the overall crystallinity as a function of the isothermal crystallization duration at (a) 110, (b) 150, and (c) 170 °C.

respectively. To determine the percentage of HC or SC contribution to the overall crystallinity, the following equations are used.

$$f_{HC} = \frac{\varphi_{c,HC}}{\varphi_{c,HC} + \varphi_{c,SC}} \times 100 \quad (5)$$

$$f_{SC} = \frac{\varphi_{c,SC}}{\varphi_{c,HC} + \varphi_{c,SC}} \times 100 \quad (6)$$

ΔH_m is a clear indicator of the amount of crystallites formed. Figure 3a–c shows that the amount of SC_1 is much smaller than HC and SC_2 and it is almost negligible. Even for the case of T_c = 170 °C where SC_1 has comparatively high ΔH_m values, it is still 5- and 13-fold lower compared to those of the SC_2 and HC cases, respectively. It is worth noting that there is a possibility of overestimating the actual value of $\Delta H_{m,SC2}$ due to the melt-recrystallization of SC_1. As for SC_2 at T_c = 110 °C, its decreasing tendency indicates the trade-off increasing of $\Delta H_{m,HC}$, suggesting the transition of the SC_2 to HC. At T_c = 150 °C, $\Delta H_{m,SC2}$ increased rapidly, reaching its maximum amount after 20 min of isothermal crystallization, before decreasing in favor of HC with the longer durations. HC formation at T_c = 150 °C took place after 5 min of isothermal crystallization and increased steadily with the longer durations, yielding the overall highest amount of HC after 300 min, with an ΔH_m value of 51.0 J/g. Unlike the case of T_c = 150 °C, $\Delta H_{m,SC2}$ at T_c = 170 °C increased slowly, reaching its maximum value after around 100 min, while SC_1 gradually increased even at a 300 min duration. With the HC appearance and its rapid growth, the ΔH_m value of SC_2 decreased, suggesting a possible conversion from SC_2 to HC. The unexpected HC formation with the long isothermal crystallization duration in the PLLA/PDLA blend, unlike the neat polymers (as shown in Figure S1b of the Supporting Information), indicates the action of SC as a powerful nucleating agent for HC. This result correlates to Xie et al. findings[26] of a highly efficient nucleation of SC kebabs on SC shish in their prepared nanofibers, while HC density was a few hundred times lower than SC. Nevertheless, HC kebabs grew more than 8 times larger compared to SC upon the thermal annealing of the nanofibers for 15 h at 70–80 °C. This may explain the long time needed for HC to form but once formed it followed a rapid growth which agrees with our results, shown by $\Delta H_{m,HC}$ tendency in Figure 3c. Based on the DSC results (for which the heating rate effect was corrected for by extrapolation to zero heating rate; see Figures S3 and S4 in the Supporting Information), we estimated the equilibrium melting temperature (T_m°) of HC, SC_1, and SC_2 at 191.2 °C, 212.3 and 226.9 °C, respectively, as shown in the Hoffman–Weeks plot in Figure 4. Here, the results at T_c = 180 °C were included, for which the DSC curve is shown in Figure S1a of the Supporting Information. The obtained T_m°s of both SC_1 and SC_2 are lower than the highest value (279 °C) reported for SC by Tsuji and Ikada.[27] In their study, they also reported T_m° ranging from 214 to 263 °C for SC in PLLA/PDLA blends and indicated its dependence on the molecular weight and optical purity of the polymer. Additionally, other studies estimate $T_{m,SC}^\circ$ within the range from 181.9 to 268.5 °C.[28−30] As for T_m° of HC, it is lower than many values reported for PLLA,[23,28,31] which are in the range of 193.3 to 198 °C. This may be due to the presence of a high D content (50%) in the blend specimen, that acts as impurity during crystallization (melting point depression). On the other hand, there may be a possibility to account for $T_{m,SC}^\circ$ = 279 °C of the highest reported value in the literature, which is by the estimation according to the broken line in Figure 4 passing through only two data points at higher crystallization temperature range, although it is erroneous ($T_{m,SC1}^\circ$ = 266.3 °C).

https://doi.org/10.1021/acsomega.3c05165
ACS Omega 2023, 8, 40482−40493

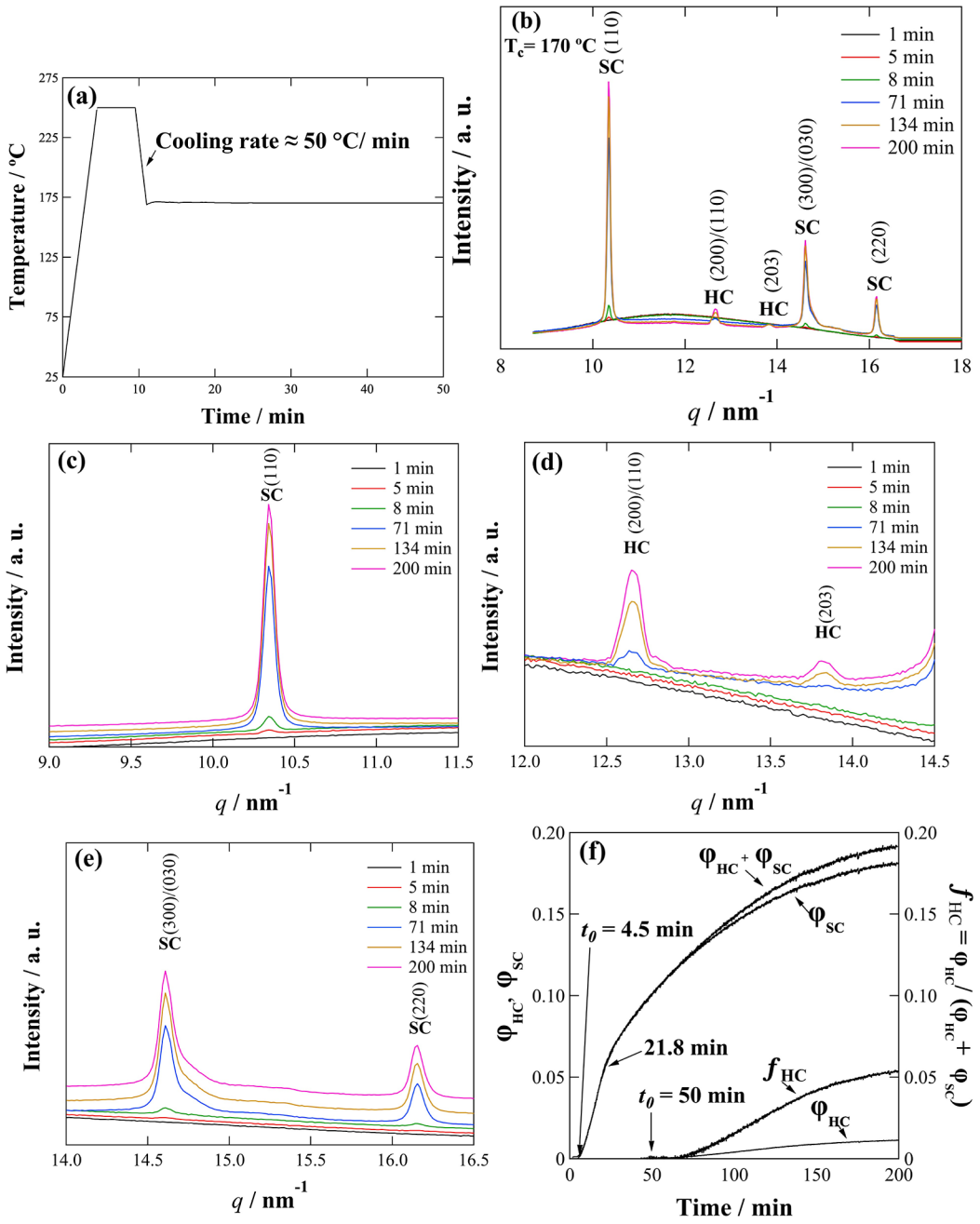

Figure 6. (a) Temperature change upon the rapid cooling for the isothermal crystallization at T_c = 170 °C upon quenching from 250 °C for the PLLA/PDLA (50/50) blend specimen, (b) the resulted changes in the WAXD profiles along the isothermal crystallization, (c), (d) and (e) close-ups of (b) showing the emergence of SC and HC peaks and (f) the temporal change of the overall degree of crystallinity (ϕ_{HC} + ϕ_{SC}) calculated from (b), the individual degrees of crystallinity of SC (ϕ_{SC}) and HC (ϕ_{HC}) and the HC contributing fraction (f_{HC}) to the overall crystallinity.

Figure 3 also shows the changes in T_m as a function of the isothermal crystallization duration. $T_{m,SC1}$ and $T_{m,SC2}$ showed no direct correlation between T_c and the crystallization duration and remained at almost the same temperature (refer to Table S1 of the Supporting Information for detailed values of T_m). This indicates that the chosen crystallization temperatures are relatively low, and the SC crystallites did not thicken. In contrast, $T_{m,HC}$ increased considerably with an increase in T_c, indicating the formation of thicker crystallites at higher crystallization temperatures. Moreover, within the same T_c, $T_{m,HC}$ increased with longer crystallization durations. It is noteworthy that the thickening of the HC crystallites took place at a crystallization temperature as high as T_c = 170 °C, although the HC crystallization was very slow because T_c = 170 °C is very close to the equilibrium melting temperature.

Figure 5 shows f_{HC}, f_{SC1}, and f_{SC2}, the contributing fractions of HC, SC_1, and SC_2, respectively, to the overall degree of crystallinity (ϕ_c) as a function of the isothermal crystallization duration. The decrease of f_{SC2} in longer durations is clearly observed in favor of f_{HC}, whereas f_{SC1} is negligible for T_c = 110 °C and absent for T_c = 150 °C. In Figure 5b, the behaviors of f_{HC} and f_{SC2} are opposite to each other, almost symmetrical with respect to 50%. Unlike T_c = 110 °C, where f_{HC} was higher for all the durations, for T_c = 150 °C, f_{SC2} decreased rapidly from 100% to its lowest value, namely, 17.3%, after 300 min. As for T_c = 170 °C, f_{SC1} had the highest values among all the

https://doi.org/10.1021/acsomega.3c05165
ACS Omega 2023, 8, 40482−40493

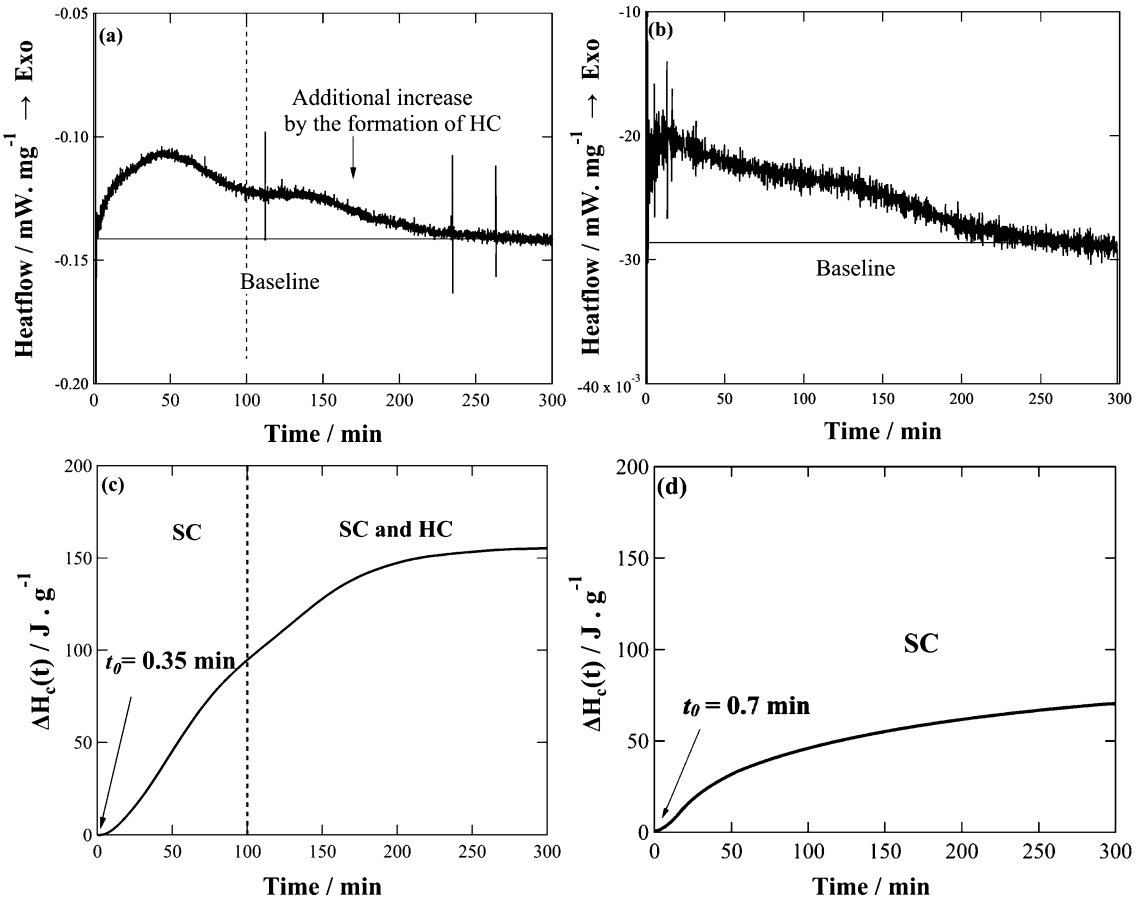

Figure 7. DSC curves during the isothermal crystallization at (a) 170 and (b) 180 °C for the PLLA/PDLA (50/50) blend specimen, and (c) and (d) the resulted $\Delta H_c(t)$.

isothermal crystallization temperatures examined in this study; it increased steadily until a 100 min duration and then decreased in favor of HC. However, the trend observed in Figure 5c indicates the long induction period of HC, within 100 min, and it surpassed SC with a contributing fraction of 56.6% (at 180 min) of the overall crystallinity.

WAXD Measurements of the PLLA/PDLA (50/50) Blend Specimens. The time-resolved WAXD results confirmed the evolution of the HC upon isothermal crystallization at T_c = 170 °C. Figure 6a demonstrates the change in temperature during the measurement (note here that the total isothermal duration was 200 min). Figure 6b shows the change in WAXD profiles for the PLLA/PDLA (50/50) blend specimen as a function of time. In Figure 6d, the emergence of the first HC diffraction peaks at q = 12.6 nm^{-1} and q = 13.8 nm^{-1} was recognized at 71 min after the temperature stabilized at 170 °C. The overall degree of crystallinity as a function of time was calculated from the WAXD profiles (Figure 6b) by the following equations:[19]

$$\varphi_{HC}=\frac{\Sigma A_{HC}}{\Sigma A_{HC}+\Sigma A_{SC}+A_a} \quad (7)$$

$$\varphi_{SC}=\frac{\Sigma A_{SC}}{\Sigma A_{HC}+\Sigma A_{SC}+A_a} \quad (8)$$

$$f_{HC}=\frac{\varphi_{HC}}{\varphi_{HC}+\varphi_{SC}} \quad (9)$$

Here A_a is the peak area of the amorphous halo. ΣA_{HC} and ΣA_{SC} are the summations of the HC and SC peak areas, respectively, while f_{HC} is the fraction contributing to the overall crystallinity. Peak decomposition analysis was carried out to distinguish amorphous and crystalline peaks, and subsequently, the degree of crystallinity as a function of time was evaluated as shown in Figure 6f. Figure 6f shows the separate degrees of crystallinity for both SC and HC, with SC being the major contributor to the overall crystallinity. Although the behavior of f_{HC} in Figure 6f (right axis) seems similar to that of f_{HC} in Figure 5c. The values in Figure 6f are much smaller compared to Figure 5c. Since the WAXD measurements can follow the in situ isothermal crystallization process, those in Figure 6f are considered to be more reliable. Then, the result of the DSC measurements giving much larger values (Figure 5c) may be ascribed to the method itself, as the DSC measurement should accompany the heating of the specimens, which are isothermally annealed (crystallized). Namely, somewhat unknown and unfavorable phenomena may take place, which are subjected to affect the evolution of the endothermic peaks, resulting in the overestimation of ΔH_m.

In addition, Figure 6b shows that the intensity increased with time for all of the peaks. This clearly indicates that both HC and SC grew simultaneously, despite the delayed formation of HC. In other words, SC crystallization did not stop after the onset of the HC crystallization. This corresponds to the primary and secondary crystallization in polymers reported by many studies.[32−34] The limited polymer chain diffusion due to the confined space between the initial SC_2 crystallites would still allow the formation of HC and additional SC, as observed in SC_1, although smaller in size,

https://doi.org/10.1021/acsomega.3c05165
ACS Omega 2023, 8, 40482−40493

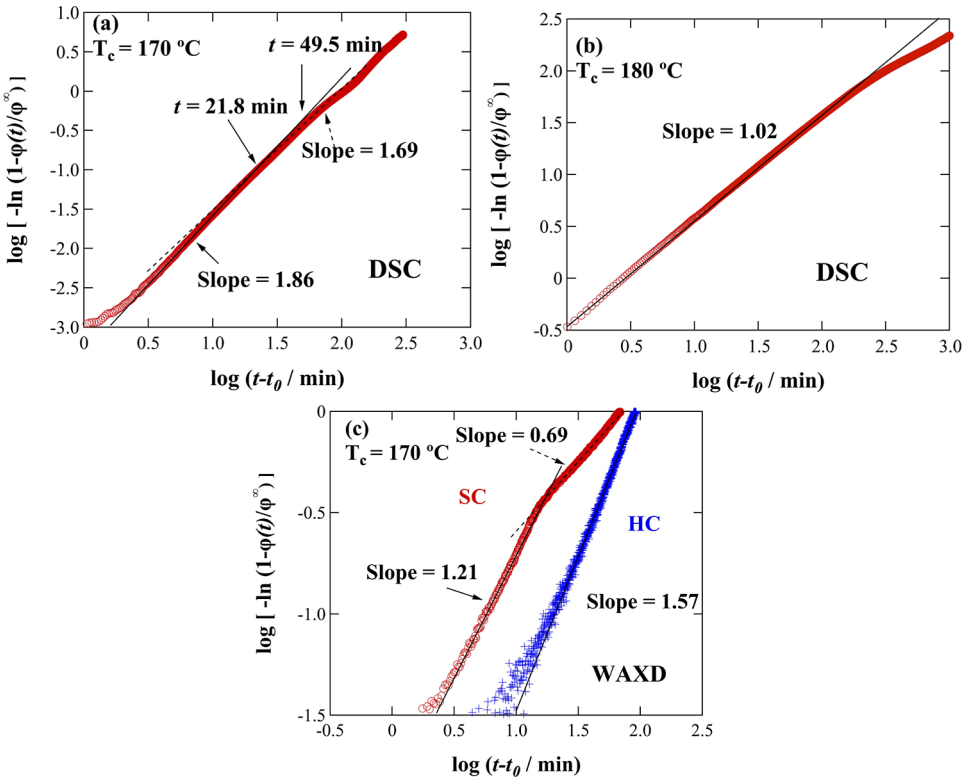

Figure 8. Avrami plots (a), (b) based on the DSC results presented in Figures 7c,d, and (c) based on the WAXD results presented in Figure 6f.

which melts at a temperature lower than SC_2. This can explain the dual melting behavior of SC, as the SC_1 melting at lower temperatures formed as a result of the secondary crystallization, restricted by the larger crystallites of SC_2 formed as a result of the primary crystallization. Note that the duality was found by numerous studies in melt-recrystallization process of crystalline polymers.[15,35,36] Furthermore, it is worth noting that the appearance of double melting peaks for the same crystalline form and the dual melting behavior of PLLA/PDLA blends were observed in many studies.[35,37] The mechanism explained for the dual formation of SC by Saeidlou et al. was based on the observation of a dual network/spherulite structure in the SC crystalline morphology.[38] However, it should be noted that what they presented about a network structure was not observed by our POM observations.

Isothermal DSC Measurement at T_C = 170 °C and T_C = 180 °C for the PLLA/PDLA (50/50) Blend Specimen. Figure 7 shows the heat flow curves during the isothermal crystallization for 300 min at T_c = 170 °C (a) and T_c = 180 °C (b), and their respective enthalpy of crystallization (ΔH_c(t)) as a function of time in parts (c) and (d). The broken lines in Figure 7a,c indicate the time when HC started to appear in the DSC curves, according to Figure 2c. The heat flow curve in Figure 7a shows two clear peaks, supposedly ascribed to the crystallization of SC and successive HC. However, as proven by WAXD, HC crystallization set in after 70 min, which was before the end of the first crystallization peak in Figure 7a. Based on this result, the crystallization curve, as shown in Figure 7c, can be compared with that shown in Figure 6f. The former is obtained by DSC measurements while the latter is obtained by WAXD measurements. Both curves show a short induction period of 2−3 min, corresponding to the one obtained from the POM observations (shown in Figure 10). In addition, Figures 7c and 6f are similar as both curves can be divided into three parts with different slopes. First, the initial part, with the highest slope, indicated the crystallite growth after quenching from the melt. Second, the middle part of both curves has a milder slope, indicating a slower crystallization due to crystallite impingement taking place. Third, the late stage of each curve exhibits the leveling-off behavior, indicating a much slower crystallization at its end. Although both curves share similar features, it is not possible to clearly distinguish between HC and SC contributions in Figure 7c. On the other hand, for the WAXD result shown in Figure 6f, both HC and SC contributions to the overall crystallinity can be recognized.

The DSC isothermal crystallization of the PLLA/PDLA (50/50) blend specimen at T_c = 180 °C was performed for 300 min. In the subsequent heating to 250 °C (shown in Figure S1a of the Supporting Information) two melting peaks were observed at 213.3 and 223 °C, being ascribed to the melting of SC_1 and SC_2, respectively, with no appearance of an HC melting peak. Unlike T_c = 170 °C, T_c = 180 °C proved to be too high for the formation of HC, despite the long isothermal crystallization duration (300 min). On the other hand, the melting temperature of SC_1 shifted to a higher temperature with the higher isothermal crystallization temperature. Note that these results were already included in the Hoffman−Weeks plot (Figure 4). Also, the WAXD results of the isothermal crystallization of the blend specimen at T_c = 180 °C (shown in Figure S2 of the Supporting Information) show SC peaks only, without the appearance of HC diffraction peaks.

Crystallization Kinetics Analyzed by Avrami Plot. To elucidate the complex crystallization behavior at T_c = 170 °C, the Avrami plot was completed based on both the WAXD and DSC results presented in Figures 6f, 7c and d, using the Avrami equation[39−41] to express the temporal evolution of the degree of crystallinity as a function of time ($\phi(t)$), as follows:

https://doi.org/10.1021/acsomega.3c05165
ACS Omega 2023, 8, 40482−40493

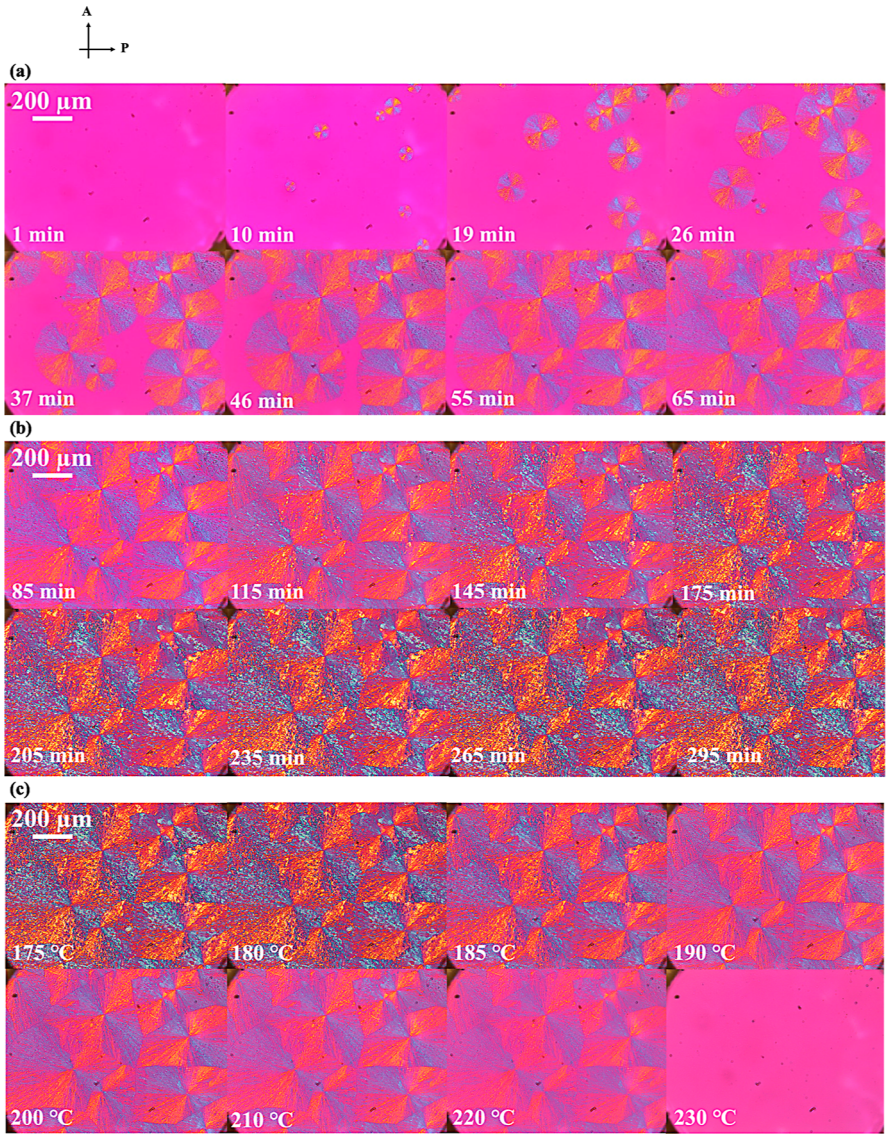

Figure 9. POM micrographs obtained (a,b) during the isothermal crystallization at 170 °C of the PLLA/PDLA (50/50) blend specimen and (c) during the subsequent heating to 250 °C.

$$\frac{\varphi(t)}{\varphi^{\infty}} = 1 - \exp[-k(t - t_0)^n] \tag{10}$$

$$\log\left[-\ln\left(1 - \frac{\varphi(t)}{\varphi^{\infty}}\right)\right] = n\log(k) + n\log(t - t_0) \tag{11}$$

where $\frac{\varphi(t)}{\varphi^{\infty}}$ is the normalized degree of crystallinity, t_0 is the induction period for the crystallization, n is the Avrami exponent, representing the dimensionality of the crystallite growth, and k is the crystallization rate constant.

Figure 8 shows the Avrami plots based on the DSC results of the PLLA/PDLA blend specimen crystallized for 300 min at T_c = 170 °C and T_c = 180 °C. In Figure 8a, the Avrami exponent (n), found from the slope, changed from 1.86 to 1.69 °C, indicating a slight change in the dimensionality of the crystal growth. The lower exponent value, approximately 3/2, may indicate an instantaneous nucleation with a crystallite growth between 1-dimensional and 2-dimensional, rod-like, or disk-like growth. While the higher exponent value, approximately 2, indicates an instantaneous nucleation with a 2-dimensional, disk-like growth. Note that the instantaneous nucleation was confirmed by POM observation (Figure 9a). The crossover time of slope change in Figure 8a is around 21.8 min, which corresponds to the inflection point of the φ_{SC} curve in Figure 6f. A similar crossover was more clearly found in Figure 8c for the SC Avrami plot. Since the crossover time (16−22 min) is well below 50 min (evolution of the HC peak in the WAXD profile; see Figure 6f), this crossover was not ascribed to the HC formation. Rather, the reason of the crossover was simply existing in the kinetics of the pure SC phase. We will consider again the meaning of this crossover later in the discussion of Figure 8c. As for Figure 8b, at T_c = 180 °C, n = 1.02 definitely indicates that the nucleation was instantaneous with a 1-dimensional (rod-like growth). It is noteworthy that the Avrami exponent depends on T_c, in this case it decreased by half with a 10 °C increase in T_c from 170 to 180 °C. Also, this 10 °C increase in T_c resulted in the doubling of t_0 from 0.35 to 0.7 min at T_c = 170 °C and T_c = 180 °C, respectively (Figure 7c,d). The decrease in the growth dimensionality and the increase in t_0 (the induction period) may be ascribed to the deceleration of the crystallization at the higher crystallization

https://doi.org/10.1021/acsomega.3c05165
ACS Omega 2023, 8, 40482−40493

temperature. Figure 8c shows the Avrami plots based on the WAXD results of the same specimen, isothermal crystallization at T_c = 170 °C. WAXD can distinguish SC and HC so that these kinetics can be independently discussed. As for SC, the crossover of the Avrami exponent from 1.21 at the early stage to 0.69 at the later stage was observed clearly at 16 min. Although the Avrami exponent values are different from those in Figure 8a, a decrease in the Avrami exponent was observed upon the crossover. Although it seems that the growth dimensionality was decreased, Avrami exponent less than unity is characteristic for the case of the lack of the crystallizable component at the growth front.[42] Namely the quick growth of SC in the earlier stage results in the lack of the crystallizable component at the growth front so that no more growth was met, and deceleration of the growth with time ($\sim t^{-1/2}$) as a result of the required diffusion of the crystallizable component may decrease the Avrami exponent value while keeping the dimensionality (rod-like growth). It is important to note that n at 180 °C in Figure 8b is 1.02 which is closer to n = 1.21 for SC at 170 °C in Figure 8c. The former result is reasonable because the DSC result can be ascribed to the formation of only SC at 180 °C. Thus, n = 1.69−1.86 in Figure 8a at 170 °C is considered an overestimation due to the contribution of HC in the DSC result at 170 °C. On the contrary, for HC, the Avrami exponent value was evaluated at 1.57 throughout the isothermal crystallization without such crossover. This is due to the very slow HC growth. The Avrami exponent of 1.57 suggests an instantaneous nucleation with the mixture of 1- and 2-dimensional crystal growth. As shown later, POM observation confirmed the confined HC crystallization inside the SC spherulites. Therefore, a 3-dimensional growth is not allowed which is in good accord with the results of the Avrami analysis.

GPC Analysis for the PLLA/PDLA (50/50) Blend Specimen. The GPC analysis revealed a decrease in the molecular weight from 1.33×10^5 to 1.16×10^5 and 1.15×10^5 after 5 h at 170 and 180 °C, respectively. This represents a 12−13% decrease, indicating a certain degree of thermal degradation. These findings also suggest that as the crystallization temperature increased, the polymer experienced further degradation.

POM Observations at T_C = 170 °C for the PLLA/PDLA (50/50) Blend Specimen. Figure 9 shows the POM images obtained during the isothermal crystallization at T_c = 170 °C for the PLLA/PDLA (50/50) blend specimen. Figure 9a shows the early stage of the crystallization process until impingement took place. Nucleation took place quickly, with many spherulites clearly visible at 10 min elapsed after the temperature stabilized at 170 °C. Spherulite growth continued for 65 min, at which all of the observed space was filled by spherulites with their distinctive Maltese cross pattern for the negative spherulites. As shown in Figure 2c and confirmed by DSC and WAXD results, these spherulites comprise SC crystallites. Figure 9b demonstrates the further change of the images with time at T_c = 170 °C after the spherulite impingement, implying the HC crystallization in the prolonged crystallization time. Figure 9c presents the images taken during the melting process from 170 to 250 °C after 300 min of isothermal crystallization, showing the fading of spherulites with an increase in temperature. A closer examination of the images at 180, 185, and 190 °C identifies a change in the spherulites sharpness. Namely, the spherulites at 180 °C exhibiting fine structures become simplified at 190 °C, while keeping the overall characteristic features of the unchanged Maltese cross pattern. This means that the HC formed within the already established SC spherulites because the $T_{m,HC}$ for this specimen is 187.5 °C. A similar result was observed by Banpean and Sakurai for PEG-confined crystallization within PLLA spherulites.[43] Figure 10 presents the plot of the spherulite diameter as a function of time, as observed by POM at T_c = 170 °C for the PLLA/PDLA (50/50) blend specimen.

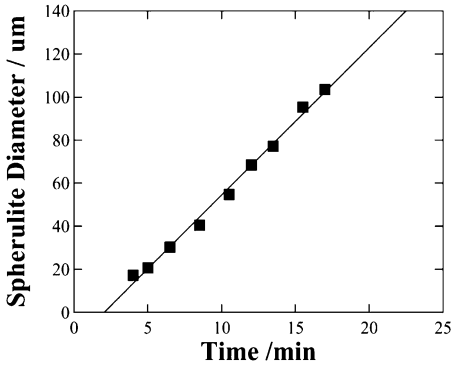

Figure 10. Plot of the spherulite diameter as a function of time, as observed by POM at T_c = 170 °C for the PLLA/PDLA (50/50) blend specimen.

spherulite diameter as a function of time. The spherulites witnessed a linear growth after an induction period of 2.02 min, with a steady diameter increase with a linear growth rate of 6.8 μm/min. Note here that both the induction period and the growth rate are deduced from the linear fitting of the observed data points.

CONCLUSIONS

The isothermal crystallization behaviors of the PLLA/PDLA (50/50) blend, neat PLLA, and neat PDLA specimens were studied at different temperatures for different durations by means of DSC, POM observations, and time-resolved WAXD. It is remarkable to observe the direct effect of the isothermal crystallization duration on the type of formed crystallites in the PLLA/PDLA (50/50) blend specimen at T_c = 170 °C. After the longer durations, HC not only formed but its melting temperature increased, resulting in significantly high melting temperature of 187.5 °C after 300 min. This T_m is more than 10 °C higher compared to the one obtained during the nonisothermal DSC measurement of the same specimen with the same heating rate in the DSC measurement. To the best of our knowledge, such a high melting temperature has never been reported before for HC of PLLA. HC did not form during the isothermal crystallization at 180 °C for the PLLA/PDLA (50/50) blend specimen nor in the isothermal crystallization at 170 °C for the neat PLLA or PDLA specimens for the same duration. In the case of the blend, HC formation is considered to be induced by the SC as a powerful nucleating agent at such a high temperature. The WAXD results confirmed that the formed crystallites with considerably long duration are ascribed to HC, not SC. Also, the POM observations indicated that HC formed within the already-established SC spherulites. According to the DSC results, $\Delta H_{m,SC2}$ showed a decreasing tendency during the isothermal crystallization duration while $\Delta H_{m,HC}$ increased instead. This may suggest a possible direct transition from SC to HC, namely, SC_2 partially melts and HC reforms.

https://doi.org/10.1021/acsomega.3c05165
ACS Omega 2023, 8, 40482−40493

■ ASSOCIATED CONTENT

Supporting Information

The Supporting Information is available free of charge at https://pubs.acs.org/doi/10.1021/acsomega.3c05165.

Isothermal DSC measurement at T_c = 170 °C for the neat specimens and at T_c = 180 °C for the blend specimen, the WAXD results for the blend at T_c = 180 °C, the effect of heating rate on the melting temperatures at different crystallization temperatures and the melting temperatures, enthalpies of fusion and contributing fractions of HC and SC for each isothermal crystallization duration (PDF)

■ AUTHOR INFORMATION

Corresponding Author

Shinichi Sakurai − *Department of Biobased Materials Science, Kyoto Institute of Technology, Kyoto 606-8585, Japan; Indian Institute of Technology Guwahati, Guwahati, Assam 781015, India;* orcid.org/0000-0002-5756-1066; Email: shin@kit.ac.jp

Authors

Neimatallah Hosni Mohammed Mahmoud − *Department of Biobased Materials Science, Kyoto Institute of Technology, Kyoto 606-8585, Japan*

Hideaki Takagi − *High Energy Accelerator Research Organization (KEK), Tsukuba, Ibaraki 305-0801, Japan;* orcid.org/0000-0003-3389-7945

Nobutaka Shimizu − *High Energy Accelerator Research Organization (KEK), Tsukuba, Ibaraki 305-0801, Japan;* orcid.org/0000-0002-3636-1663

Noriyuki Igarashi − *High Energy Accelerator Research Organization (KEK), Tsukuba, Ibaraki 305-0801, Japan*

Complete contact information is available at: https://pubs.acs.org/10.1021/acsomega.3c05165

Notes

The authors declare no competing financial interest.

■ ACKNOWLEDGMENTS

This study was supported by Japan Science and Technology Agency JST Grant Number JPMJPF2114. The WAXD experiments were performed under the approval of the Photon Factory (High Energy Research Organization, Tsukuba, Japan) Program Advisory Committee (proposal no: 2020G520).

■ REFERENCES

(1) de Sousa, F. D. B. Plastic and Its Consequences during the COVID-19 Pandemic. *Environ. Sci. Pollut. Res. Int.* **2021**, *28* (33), 46067−46078.

(2) Parashar, N.; Hait, S. Plastics in the Time of COVID-19 Pandemic: Protector or Polluter? *Sci. Total Environ.* **2021**, *759*, 144274.

(3) Sin, L. T. *Polylactic Acid: PLA Biopolymer Technology and Applications*; William Andrew Publishing, 2012.

(4) Ikada, Y.; Jamshidi, K.; Tsuji, H.; Hyon, S. H. Stereocomplex formation between enantiomeric poly(lactides). *Macromolecules* **1987**, *20* (4), 904−906.

(5) Sin, L. T.; Tueen, B. S. *Polylactic Acid A Practical Guide for the Processing, Manufacturing, and Applications of PLA*; William Andrew Publishing, 2019.

(6) Yin, H. Y.; Wei, X. F.; Bao, R. Y.; Dong, Q.; Liu, Z.; Yang, W.; Xie, B.; Yang, M. Enhancing Thermomechanical Properties and Heat Distortion Resistance of Poly(l-lactide) with High Crystallinity under High Cooling Rate. *ACS Sustain. Chem. Eng.* **2015**, *3* (4), 654−661.

(7) Zhang, Y.; Wang, Y.; Wang, B.; Feng, X.; Ma, B.; Sui, X. Exclusive Formation of Poly(lactide) Stereocomplexes with Enhanced Melt Stability via Regenerated Cellulose Assisted Pickering Emulsion Approach. *Compos. Commun.* **2022**, *32*, 101138.

(8) Luo, F.; Fortenberry, A.; Ren, J.; Qiang, Z. Recent Progress in Enhancing Poly(Lactic Acid) Stereocomplex Formation for Material Property Improvement. *Front. Chem.* **2020**, *8*, 688.

(9) Bao, R. Y.; Yang, W.; Jiang, W. R.; Liu, Z. Y.; Xie, B. H.; Yang, M. B. Polymorphism of Racemic Poly(l- lactide)/Poly(d-lactide) Blend: Effect of Melt and Cold Crystallization. *J. Phys. Chem. B* **2013**, *117* (13), 3667−3674.

(10) Han, L.; Pan, P.; Shan, G.; Bao, Y. Stereocomplex Crystallization of High-Molecular-Weight Poly(l- lactic acid)/poly-(d-lactic acid) Racemic Blends Promoted by a Selective Nucleator. *Polymer* **2015**, *63*, 144−153.

(11) Thi Ngoc Diep, P.; Mochizuki, M.; Doi, M.; Takagi, H.; Shimizu, N.; Igarashi, N.; Sasaki, S.; Sakurai, S. Effects of a Special Diluent as an Agent of Improving the Crystallizability of Poly(L-lactic acid). *Polym. J.* **2019**, *51*, 283−294.

(12) Bao, R.; Yang, W.; Wei, X.; Xie, B.; Yang, M. Enhanced Formation of Stereocomplex Crystallites of High Molecular Weight Poly(l-lactide)/Poly(d-lactide) Blends from Melt by Using Poly-(ethylene glycol). *ACS Sustain. Chem. Eng.* **2014**, *2* (10), 2301−2309.

(13) Diao, X.; Chen, X.; Deng, S.; Bai, H. Substantially Enhanced Stereocomplex Crystallization of Poly(L-Lactide)/Poly(D-Lactide) Blends by the Formation of Multi-Arm Stereo-Block Copolymers. *Crystals* **2022**, *12* (2), 210.

(14) Zhu, J.; Na, B.; Lv, R.; Li, C. Enhanced Stereocomplex Formation of High-Molecular-Weight Polylactides by Gelation in an Ionic Liquid. *Polym. Int.* **2014**, *63* (6), 1101−1104.

(15) Xu, C.; Zhang, J.; Bai, J.; Ding, S.; Wang, X.; Wang, Z. Two-Stage Crystallization Kinetics and Morphological Evolution with Stereocomplex Crystallite-Induced Enhancement for Long-Chain Branched Polylactide/Poly(D-lactic acid) Blends. *Ind. Eng. Chem. Res.* **2021**, *60* (14), 5319−5329.

(16) Feng, L.; Bian, X.; Li, G.; Chen, X. Thermal Properties and Structural Evolution of Poly(L-lactide)/ Poly(D-lactide) Blends. *Macromolecules* **2021**, *54* (21), 10163−10176.

(17) Xiong, Z.; Zhang, X.; Wang, R.; de Vos, S.; Wang, R.; Joziasse, C. A. P.; Wang, D. Favorable Formation of Stereocomplex Crystals in Poly(L-lactide)/ poly(D-lactide) Blends by Selective Nucleation. *Polymer* **2015**, *76*, 98−104.

(18) Pan, P.; Bao, J.; Han, L.; Xie, Q.; Shan, G.; Bao, Y. Stereocomplexation of High-Molecular-Weight Enantiomeric Poly-(lactic acid)s Enhanced by Miscible Polymer Blending with Hydrogen Bond Interactions. *Polymer* **2016**, *98*, 80−87.

(19) Pandey, A. K.; Takagi, H.; Igarashi, N.; Shimizu, N.; Sakurai, S. Enhanced Formation of Stereocomplex Crystallites in Poly(L-lactic acid)/ Poly(D-lactic acid) Blends by Silk Fibroin Nanodisc. *Polymer* **2021**, *229*, 124001.

(20) Zhao, N.; Wang, L.; Huang, D.; Zhang, T.; Zhang, L.; Xiong, C. Effect of Isothermal Annealing on Degree of Crystallinity and Mechanical Properties of Poly(l-lactide-co-glycolide). *Cryst. Res. Technol.* **2010**, *45* (3), 275−280.

(21) Saeidlou, S.; Huneault, M. A.; Li, H.; Park, C. B. Poly(lactic acid) Crystallization. *Prog. Polym. Sci.* **2012**, *37* (12), 1657−1677.

(22) Jamshidi, K.; Hyon, S.-H.; Ikada, Y. Thermal Characterization of Polylactides. *Polymer* **1988**, *29* (12), 2229−2234.

(23) Nijenhuis, A. J.; Colstee, E.; Grijpma, D. W.; Pennings, A. J. High Molecular Weight Poly(l-lactide) and Poly(ethylene oxide) Blends: Thermal Characterization and Physical Properties. *Polymer* **1996**, *37* (26), 5849−5857.

(24) Tsuji, H.; Ikada, Y. Properties and Morphologies of Poly(l-lactide): 1. Annealing Condition Effects on Properties and Morphologies of Poly(l-lactide). *Polymer* **1995**, *36* (14), 2709−2716.

(25) Tsuji, H.; Horii, F.; Nakagawa, M.; Ikada, Y.; Odani, H.; Kitamaru, R. Stereocomplex Formation between Enantiomeric

Poly(lactic acid)s. 7. Phase Structure of the Stereocomplex Crystallized from a Dilute Acetonitrile Solution as Studied by High-Resolution Solid-State Carbon-13 NMR Spectroscopy. *Macromolecules* **1992**, *25* (16), 4114−4118.
(26) Xie, Q.; Chang, X.; Qian, Q.; Pan, P.; Li, C. Y. Structure and Morphology of Poly(lactic acid) Stereocomplex Nanofiber Shish Kebabs. *ACS Macro Lett.* **2020**, *9*, 103−107.
(27) Tsuji, H.; Ikada, Y. Crystallization from the melt of poly(lactide)s with different optical purities and their blends. *Macromol. Chem. Phys.* **1996**, *197*, 3483−3499.
(28) Guo, W.; Shao, J.; Ye, X.; Sun, P.; Meng, C.; Li, Z.; Zheng, Z.; Yan, C. The Difference of Equilibrium Melting Point between Poly(l-lactic acid) and Poly(l-lactic acid)/poly(d-lactic acid) Blends: Cases with Three Molecular Weights. *Polym. Int.* **2019**, *68* (2), 271−276.
(29) Tsuji, H.; Matsumura, N. Stereocomplex Crystallization of Star-Shaped 4-Armed Equimolar Stereo Diblock Poly(lactide)s with Different Molecular Weights: Isothermal Crystallization from the Melt. *Macromol. Chem. Phys.* **2016**, *217* (14), 1547−1557.
(30) Rahaman, M. H.; Tsuji, H. Isothermal Crystallization and Spherulite Growth Behavior of Stereo Multiblock Poly(lactic acid)s: Effects of Block Length. *J. Appl. Polym. Sci.* **2013**, *129* (5), 2502−2517.
(31) Pandey, A. K.; Katiyar, V.; Sasaki, S.; Sakurai, S. Accelerated Crystallization of Poly(l-lactic acid) by Silk Fibroin Nanodisc. *Polymer* **2019**, *51* (11), 1173−1180.
(32) Rybnikář, F. Secondary Crystallization of Polymers. *J. Polym. Sci.* **1960**, *44* (144), 517−522.
(33) Yagpharov, M. Thermal Analysis of Secondary Crystallization in Polymers. *J. Therm. Anal.* **1986**, *31*, 1073−1082.
(34) Androsch, R.; Schick, C.; Di Lorenzo, M. L. Kinetics of Nucleation and Growth of Crystals of Poly(l-lactic acid). In *Synthesis, Structure and Properties of Poly(lactic acid)*; Di Lorenzo, M., Androsch, R., Eds.; Advances in Polymer Science; Springer: Cham, 2017; Vol. *279*, p 235.
(35) Hu, X.; Shao, J.; Zhou, D.; Li, G.; Ding, J.; Chen, X. Microstructure and Melting Behavior of A Solution-Cast Polylactide Stereocomplex: Effect of Annealing. *J. Appl. Polym. Sci.* **2017**, *134* (12), 44626.
(36) Yasuniwa, M.; Tsubakihara, S.; Sugimoto, Y.; Nakafuku, C. Thermal Analysis of the Double-Melting Behavior of Poly(L-lactic acid). *J. Polym. Sci., Part B: Polym. Phys.* **2004**, *42* (1), 25−32.
(37) Gracia-Fernandez, C. A.; Gomez-Barreiro, S.; López-Beceiro, J.; Naya, S.; Artiaga, R. New approach to the Double Melting Peak of Poly(l-lactic acid) Observed by DSC. *J. Mater. Res.* **2012**, *27* (10), 1379−1382.
(38) Saeidlou, S.; Huneault, M. A.; Li, H.; Sammut, P.; Park, C. B. Evidence of a Dual Network/Spherulitic Crystalline Morphology in PLA Stereocomplexes. *Polymer* **2012**, *53* (25), 5816−5824.
(39) Avrami, M. Kinetics of phase change. I General Theory. *J. Chem. Phys.* **1939**, *7* (12), 1103−1112.
(40) Avrami, M. Kinetics of Phase Change. II Transformation-Time Relations for Random Distribution of Nuclei. *J. Chem. Phys.* **1940**, *8* (2), 212−224.
(41) Avrami, M. Kinetics of Phase Change. III: Granulation, Phase Change and Microstructure. *J. Chem. Phys.* **1941**, *9*, 177−184.
(42) Schultz, J. M. *Polymer Crystallization: The Development of Crystalline Order in Thermoplastic Polymers*; American Chemical Society, 2001.
(43) Banpean, A.; Sakurai, S. Confined Crystallization of Poly-(ethylene glycol) in Spherulites of Poly(L- lactic acid) in a PLLA/PEG Blend. *Polymer* **2021**, *215*, 123370.

https://doi.org/10.1021/acsomega.3c05165
ACS Omega 2023, 8, 40482−40493